SDC-93-419

SDC
SOLENOIDAL DETECTOR NOTES

PARTICLE HIT RATES AT THE MUON DETECTOR

Hiroyuki Iwasaki
KEK, National Laboratory for High Energy Physics

July 5-August 1, 1992
Rocky Mountian Consortium Summer Workshops I
Boulder, Colorado

Particle Hit Rates at the Muon Detector

Hiroyuki Iwasaki

KEK, National Laboratory for High Energy Physics
Tsukuba, Ibaraki, 305 Japan

Abstract

Particle hit rates at the muon chambers of the SDC detector under the nominal SSC luminosity of 10^{33} $cm^{-2}s^{-1}$ are estimated. Particle sources considered are muons from charm and bottom decays, muons from pion and kaon decays, punchthrough particles, and cosmic-ray muons.

Talk presented at the Rocky Mountain Consortium Summer Workshops I
Physics & Detectors at the SSC
July 5 - August 1, 1992, Boulder, Colorado

1. Introduction

Particle hit rates at the muon chambers of the SDC detector (Fig.1)[1] under the nominal SSC luminosity of 10^{33} $cm^{-2}s^{-1}$ are estimated. Muon chamber BW1 (BW2) is set in front of (behind) the barrel toroid; FW1 (FW4) is set just behind the calorimeter (the forward toroid, FT2). In the estimation, we assume that the calorimeter is made of iron only and its thickness is 10 λ independent of pseudorapidity ($\eta = -\ln(\tan(\theta/2))$). Although the toroid magnets are actually octagonal, we also simplify them to be cylindrical. Particle sources considered here are muons from charm and bottom decays (prompt muons), muons from pion and kaon decay (decay muons), punchthrough particles, and cosmic-ray muons. Except for the cosmic rays, we use PYTHIA5.3 [2] at the SSC energy, $\sqrt{s}$ = 40 TeV, for the event generation. We choose the "QCD high-pt processes (MSEL=1)" as the physics processes, cross section of which is 96 mb. At the design luminosity, 1nb corresponds to 1 Hz. A summary of the hit rates is given in Table 1.

Table 1
Summary of muon hit rates at $L = 10^{33}$ $cm^{-2}s^{-1}$.

Particle	Hit rate	Area (η range)
1. Prompt μ	120 kHz	at BW1 ($\lvert\eta\rvert$ <1.3)
	55 kHz	at BW2+IW2 ($\lvert\eta\rvert$ <1.5)
	120 kHz / end	at FW1 (1.3 <η < 2.5)
	39 kHz / end	at FW4 (1.6 <η < 2.5)
2. Decay μ	640 kHz	at BW1 ($\lvert\eta\rvert$ <1.3)
	54 kHz	at BW2+IW2 ($\lvert\eta\rvert$ <1.5)
	4.9 MHz / end	at FW1 (1.3 <η < 2.5)
	140 kHz / end	at FW4 (1.6 <η < 2.5)
3. Punchtrough	180 kHz	at BW1 ($\lvert\eta\rvert$ <1.3)
	0.2 kHz	at BW2+IW2 ($\lvert\eta\rvert$ <1.5)
4. Cosmic ray	19 kHz	at BW2+IW2 ($\lvert\eta\rvert$ <1.5)
Total	940 kHz	at BW1 ($\lvert\eta\rvert$ <1.3)
	130 kHz	at BW2+IW2 ($\lvert\eta\rvert$ <1.5)
	≥ 5.0 MHz / end	at FW1 (1.3 <η < 2.5)
	≥ 180 kHz / end	at FW4 (1.6 <η < 2.5)

Hits due to neutrons or electromagnetic debris associated with a high energy muon are not considered in this report. Except for integrated rates for prompt and decay muons, contents are basically the same as given in ref.[3].

2. Prompt muons

2.1. Characteristics

Prompt muons are the decay muons from the heavy-quark (charm, bottom) hadrons. Differential cross section in the the central region ($|\eta| < 1.4$) versus p_t is shown in Fig.2, where p_t is the transverse momentum of the muon at the interaction region. The generated points in the region of $p_t > 10$ GeV/c are well fitted with a function,

$$\frac{d\sigma}{dp_t\, d\eta} = \frac{9.12\text{x}10^7}{p_t{}^{4.87}}$$

where $d\sigma/dp_t\, d\eta$ is given in nb/GeV/c and p_t in GeV/c. Compared with a distribution given in ref.[4], where generated data points are plotted up to 1 TeV/c, the formula is consistent up to about 300 GeV/c (see Fig.3).

Pseudorapidity distribution is shown in Fig.4 for any prompt muons, and those with p_t larger than 1 GeV/c or 2 GeV/c. Indeed the distribution becomes slightly narrower as the p_t increases, the pseudorapidity distribution is almost flat in the muon system ($|\eta| < 2.5$). Multiplicity distribution of the prompt muons which enter the central region ($|\eta| < 1.4$) is plotted in Fig.5 for several p_t-cut values. Rate of prompt muons with any p_t emitted in this region is about 1 particle per 100 QCD events. The rate decreases by approximately one order of magnitude for additional multiplicity increment. With p_t-cut of 2 GeV/c, the rate is 1 particle per 1000 events; it decreases by more than two orders with additional multiplicity.

2.2. Hit rates

We parametrize the $d\sigma/dp_t\, d\eta$ distribution as shown with solid line in Fig.6. Integrated cross section in the central region, $d\sigma/d\eta$, versus p_t-threshold is shown in Fig.7. Material thickness up to the chambers in interaction length as a function of pseudorapidity is plotted in

Table 2
Summary of hit rates due to prompt muons at $L = 10^{33}$ cm^{-2}s^{-1}.

Particle	Hit rate	Area (η range)
Prompt μ	34 kHz /η	at BW1 (averaged over $\lvert\eta\rvert<1.4$)
per unit η	14 kHz /η	at BW2 (averaged over $\lvert\eta\rvert<1.4$)
Prompt μ	120 kHz	at BW1 ($\lvert\eta\rvert<1.3$)
integrated rate	55 kHz	at BW2+IW2 ($\lvert\eta\rvert<1.5$)
	120 MHz / end	at FW1 ($1.3<\eta<2.5$)
	39 kHz / end	at FW4 ($1.6<\eta<2.5$)

Fig.8. Note that the thickness of the calorimeter and the other materials inside is assumed to be 10 λ independent of η. Each iron toroidal magnet is 1.5 m in thickness. Muon range in iron versus its momentum is plotted in Fig.9. At $\eta = 0$, only muons with momenta greater than 2.2 GeV/c can pass through the calorimeter (10 λ); minimum momentum of 4.3 GeV/c is required to reach BW2.

Minimum p_t required to penetrate the calorimeter or the iron toroid as a function of η is plotted in Fig.10. In order to estimate the integrated hit rates, we parametrize the pseudorapidity distribution as shown with solid line in Fig.11. Convoluting $d\sigma/dp_t\, d\eta$ in the central region and $(dN/d\eta)/N$, and integrating it from minimum-p_t to infinity, we get $d\sigma/d\eta$ as a function of η. In Fig.12a (12b), we show the cross section of prompt muons to hit BW1 or FW1 (BW2, IW2 or FW4) with solid line. The hit rate per unit rapidity at BW1 (averaged over $\lvert\eta\rvert < 1.4$) is estimated to be 34 kHz; it decreases down to 14 kHz at BW2. We get the hit rates in each detector region by integrating the cross section over η, which are summarized in Table 2. The rates are 120 kHz at BW1 ($\lvert\eta\rvert < 1.3$) and 55 kHz at BW2/IW2 ($\lvert\eta\rvert < 1.5$).

3. Decay muons

3.1. Characteristics

Decay muons are the decay products from charged pions and kaons in flight. As for the decay volume, we assume a radius of 1.7 m and a half length of 4 m. Differential cross section in the the central region ($\lvert\eta\rvert < 1.4$) versus p_t is shown in Fig.13, where p_t is the transverse

momentum of the muon inside the decay volume. The generated points above 1 GeV/c, are well fitted with a function,

$$\frac{d\sigma}{dp_t\, d\eta} = \frac{5.08\times 10^6}{p_t{}^{4.62}}$$

where $ds/dp_t\, d\eta$ is given in nb/GeV/c and p_t in GeV/c.

Pseudorapidity distribution is shown in Fig.14 for any prompt muons, and those with p_t larger than 1 GeV/c or 2 GeV/c. Compared to that of prompt muons, it is a much narrower distribution. It is because the decay probability of kaons or pions is approximately proportional to $\tan\theta/p_t$ (= $1/p_t \sinh\eta$) in the forward region for $p_t >> m_\pi$ or m_K, and therefore it decreases exponentially as η in this region for fixed p_t. On the other hand, it is approximately proportional to $1/p_t$ and independent of θ in the barrel region. Multiplicity distribution of the decay muons which enter the barrel region ($|\eta| < 1.4$) is plotted in Fig.15 for several p_t-cut values. About 80% of QCD events have decay muons with any p_t emitted in this region. However, most of their p_t values are small. With p_t-cut of 2 GeV/c, the multiplicity is approximately 1 particle every 400 QCD events; the rate decreases by more than two orders of magnitude for additional multiplicity increment.

3.2. Hit rates

Following the similar procedure as for the prompt muons, we parametrize the $d\sigma/dp_t\, d\eta$ distribution as shown with dashed line in Fig.6; its integrated cross section versus p_t-threshold in Fig.7; pseudorapidity distribution in Fig.11; $d\sigma/d\eta$ as a function of η in Fig.12. Averaged

Table 3
Summary of hit rates due to decay muons at $L = 10^{33}$ cm^{-2}s^{-1}.

Particle	Hit rate	Area (η range)
Decay μ	78 kHz /η	at BW1 (averaged over $|\eta|<1.4$)
per unit η	7.2 kHz /η	at BW2 (averaged over $|\eta|<1.4$)
Decay μ	640 kHz	at BW1 ($|\eta|<1.3$)
integrated rate	54 kHz	at BW2+IW2 ($|\eta|<1.5$)
	4.9 MHz / end	at FW1 ($1.3<\eta<2.5$)
	144 kHz / end	at FW4 ($1.6<\eta<2.5$)

over $|\eta| < 1.4$, the hit rate per unit rapidity is estimated to be 78 kHz at BW1 and 7.2 kHz at BW2. The integrated hit rates are 640 kHz at BW1 ($|\eta| < 1.3$) and 54 kHz at BW2+IW2 ($|\eta| < 1.5$). These results are summarized in Table 3.

4. Punchthrough

As for the punchthrough properties through the calorimeter and the ion toroid, we use the parametrization developed by R.McNeil *et al.*[5]. In the parametrization, the punchthrough probability is based on experimental data taken by the CCFR neutrino detector [6], and the exit angle and position distributions are based on the GEANT simulation. We neglect a effect coming from the spacing between the calorimeter and the chambers. The resultant hit rates are summarized in Table 4. The punchthrough hit rate integrated over the whole BW1 ($|\eta| < 1.3$) is 180 kHz. The corresponding hit rate over the BW2 and IW2 ($|\eta| < 1.5$) is only 180 Hz.

Table 4
Summary of hit rates due to punchtrough particles in the barrel region at $L = 10^{33}$ cm^{-2}s^{-1}.

Particle	Hit rate	Area (η range)
Punchtrough	180 kHz	at BW1 ($|\eta| <1.3$)
	180 Hz	at BW2+IW2 ($|\eta| <1.5$)

5. Cosmic rays

We use a formula given in ref.[7] for the flux of cosmic rays at the sea level. Differential flux in the vertical direction calculated with the formula is plotted in Fig.16 together with experimental data points (ref.[8]). Although the formula gives slightly lower flux below 2 GeV/c, it reproduces the data points satisfactory. Since the experimental hall is underground and we care about cosmic rays with momenta grater then 4 GeV/c, the discrepancy is no problem at all in practice. In an estimation, we simplify the experimental hall as an infinitely long square tunnel as shown in Fig.17. We assume the density of the soil around the experimental hall to be 2.0 g/cm^3, and a constant energy loss of 2 MeV/(g/cm^2) for cosmic rays. The hit rates on the top octant of BW2 and on the octant next to the top are about 8 kHz and 5

kHz, respectively. It is less than 1 kHz for the side octant. The hit rate on the entire region on IW2 is 0.2 kHz per end. Thus, the total cosmic ray rate is 19.3 kHz in the barrel and intermediate region ($|\eta| < 1.5$). These hit rates are summarized in Table 5.

Table 5
Summary of hit rates in the barrel region due to cosmic rays.

Particles	Hit rate	Area (η range)
Cosmic ray	8.2 kHz / octant	at the top octant of BW2($|\eta|<1.3$)
	4.8 kHz / octant	at octant next to the top
	0.6 kHz / octant	at side octant
	0.2 kHz /end	at IW2 ($1.3<|\eta|<1.5$)
Total	19.3 kHz	at BW2+IW2 ($|\eta|<1.5$)

5. Summary

The hit rate at each area is summarized in Table 1. In the barrel region, the total hit rates are approximately 1 MHz at BW1 ($|\eta| < 1.3$) and 130 kHz at BW2+IW2 ($|\eta| < 1.5$). At BW1, decay muons (640 kHz) is the dominant source; hit rates due to prompt muons (120 kHz) and punchtrough particles (180 kHz) are the same level, each of which is about factor 4 to 5 smaller than that of decay muons. At BW2+IW2, contributions from prompt muons (55 kHz) and decay muons (54 kHz) are the same. Although the total cosmic ray rate is about factor 3 smaller than each of these muon rates, the contribution is even larger at the top octant of BW2 (8.2 kHz) than prompt muons (5.3 kHz) or decay muons (3.6 kHz). Of course, this argument depends on the actual depth of the experimental hall in the underground. Hits due to punchthrouh is negligibly small behind the barrel toroid (180 Hz).

In the forward region, we estimate the contributions from prompt muons and decay muons only. The hit rates per each end due to these muons are about 5 MHz at FW1 ($1.3 <\eta < 2.5$) and 140 kHz at FW4 ($1.6 <\eta < 2.5$). At both locations, the contribution from decay muons is dominant. Especially at FW1, it is 40 times larger than that of prompt muons. Compared to the prompt muons, decay muons show a steep rise towards the edge of the muon system even as a function of η (Fig.12). One should note that a small change of p_t-cut on the muon range result in a large difference in hit rate due to decay muons (Fig.7): 10% smaller p_t-cut corresponds to

30 - 40 % increase in hit rate at around p_t-cut of 0.4 GeV/c. Therefore, the hit rates due to decay muons in the forward region should be treated as rough values.

References

[1] SDC collaboration, *TECHNICAL DESIGN REPORT*, SDC-92-201, April 1992.

[2] H.-U. Bengtsson and T.Sjöstrand, Computer Physics Commun. **46** (1987) 43.

[3] Y. Arai, Y. Asano, K. Fujita, Y. Funahashi, Y. Higashi, H. Iwasaki, N. Kanematsu, T. Kondo, A. Maki, S. Mori , S. Odaka, T. Okusawa, H. Sakamoto, T. Shinkawa T. Takahashi, S. Terada, Y. Teramoto and T. Yoshida, "Conceptual Design Report for the SDC Barrel and Intermediate Muon Detectors Based on a Jet-type Drift Chamber", KEK Report 92-1, SDC-92-169, April 1992.

[4] F.E. Paige, "SSC Trigger Cross Sections" page 51, in Proceedings of the Workshop on Triggering, Data Acquisition and Computing For High Energy/High Luminosity Hadron-Hadron Colliders, Fermilab, November 1985, edited by B. Cox, R. Fenner and P. Hale.

[5] R.McNeil, W.Morse and H.Ma, private communication. Since we used an old version, the program unfortunately returned probability of zero for hadrons with momenta less than 100 GeV/c for material thickness greater than 19.2 λ. In the region where the probability becomes less than 0.2%, we used the empirical formula by Lang (K.Lang, Rochester Report No. UR890 ER13065-409 (1985); A.Bodek, UR911 ER13065-412 (1985)).

[6] F.S. Merritt et al., Nucl. Instr. and Meth. A245 (1986) 27.

[7] W.D. Dau, K. Carstensen and H. Jokisch, Proc. 14th Int. Conf. on Cosmic Rays, Munchen, MN page 1931, 1974. The formula in the original article is given for large zenith angles (>79 deg) and a correction for the spherical surface of the earth is made. Since it is not necessary for the present study, the correction is ignored. The parameter values given in the formula are tuned up to reproduce data better in the small zenith angle region.

[8] O.C. Allkofer, K. Carstensen and W.D. Dau, Proc. 12th Int. Conf. on Cosmic Rays, Hobart, Tasmania, MU page 1314, 1971.

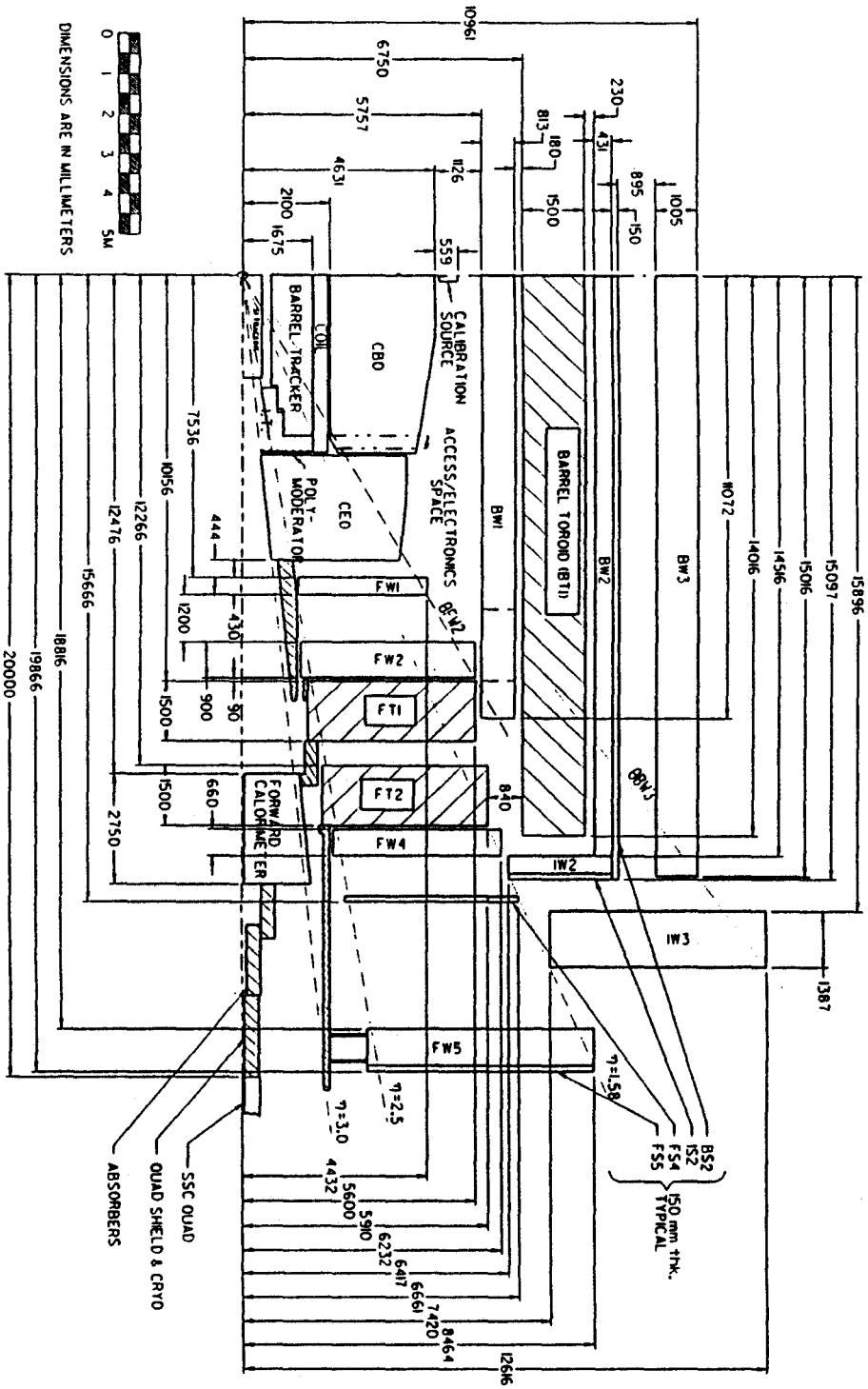

Fig.1. Layout of the SDC muon system. BW, IW and FW stand for barrel, intermediate and forward wire chamber, respectively. Each of the barrel toroid (BT1), forward toroids (FT1 and FT2) is made of iron and 1.5 m in thickness.

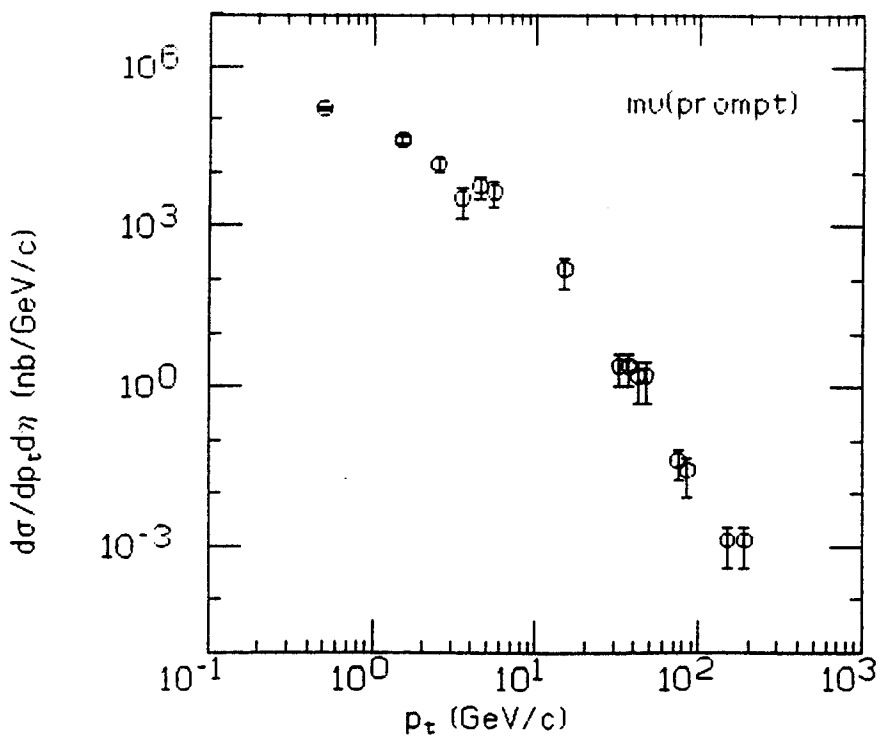

Fig.2. Differential cross section, $d\sigma/dp_t\, d\eta$, as a function of p_t for prompt muons. Events are generated by using PYTHIA5.3.

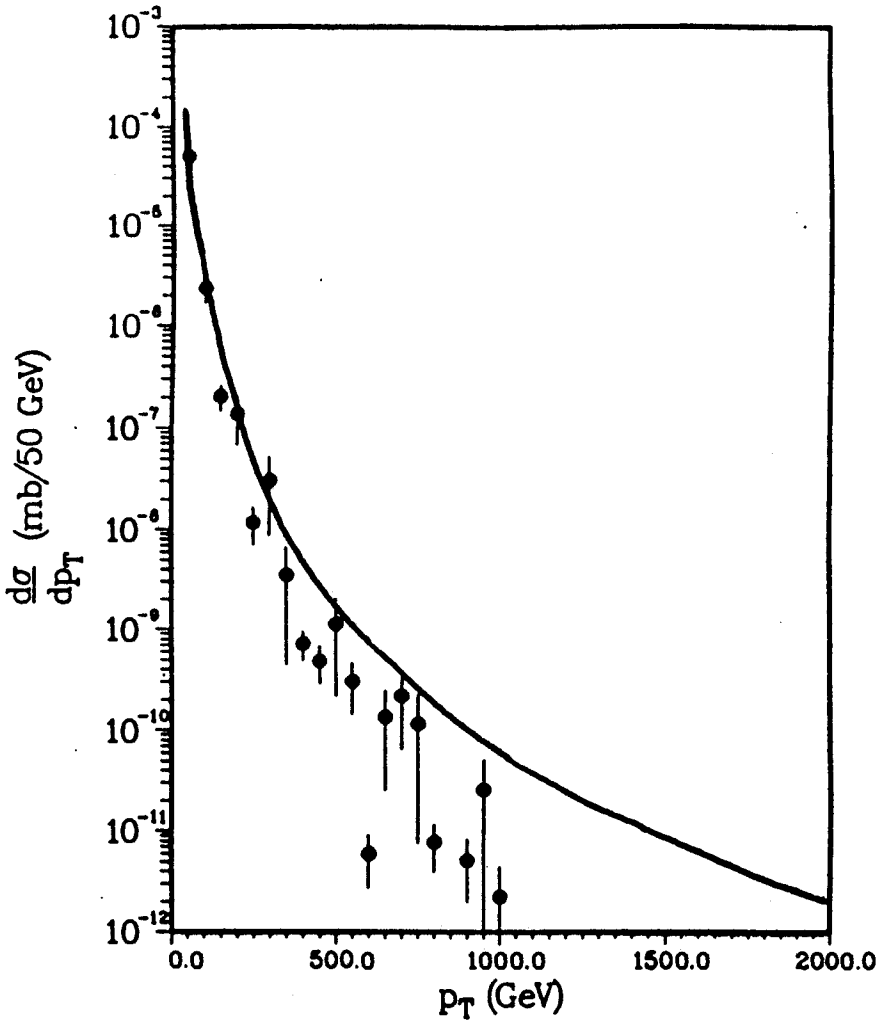

Fig.3. Differential cross section, $d\sigma/dp_t$, as a function of p_t for prompt muons (ref.[4]). Solid line is the parametrization given in the text, where η interval is taken to be 6.

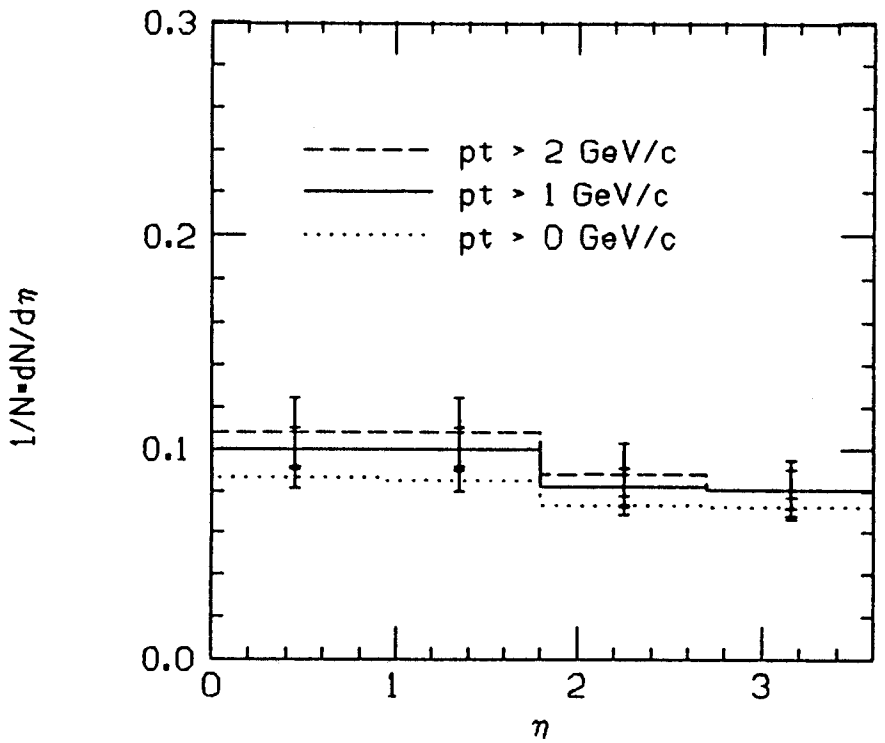

Fig.4. Pseudorapidity distribution for any prompt muons (dotted line), those with p_t larger than 1 GeV/c (solid line) or 2 GeV/c (dashed line).

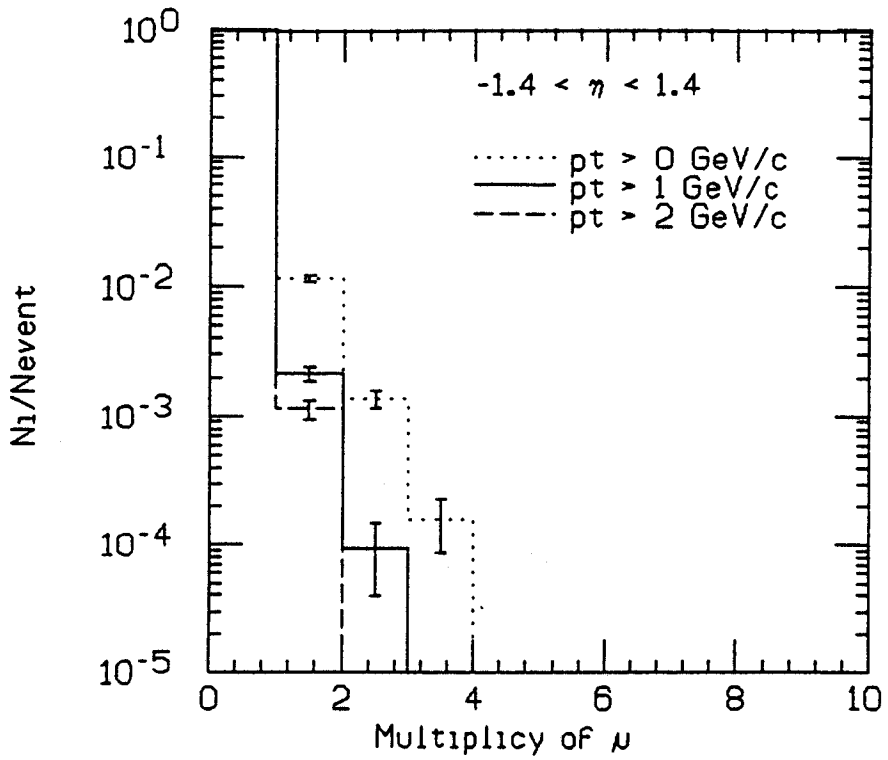

Fig.5. Multiplicity distribution of prompt muons which enter the central region ($|\eta| < 1.4$) for any prompt muons (dotted line), those with p_t larger than 1 GeV/c (solid line) or 2 GeV/c (dashed line).

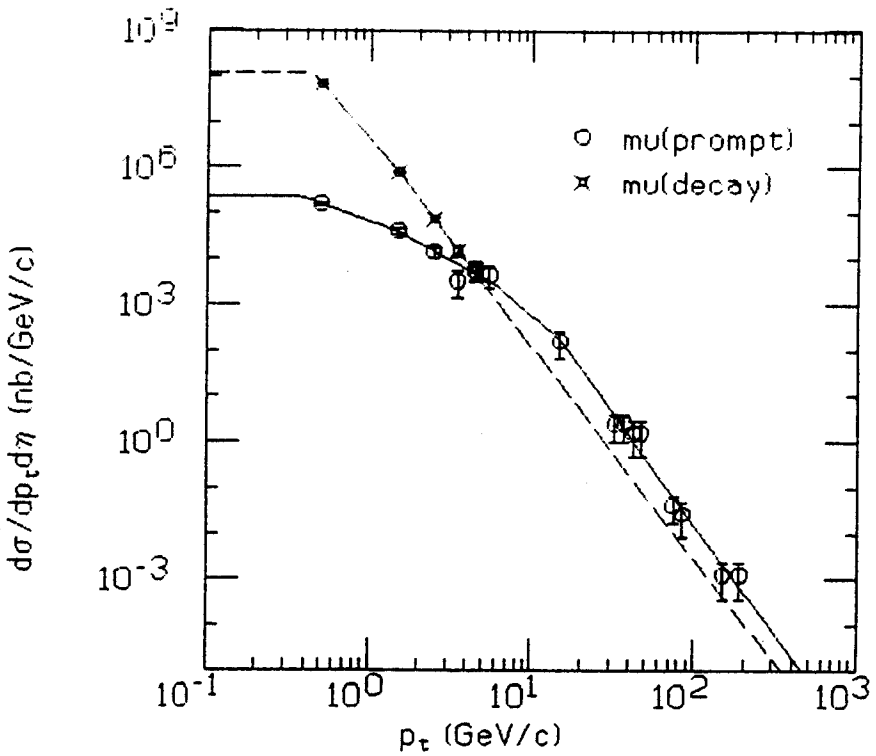

Fig.6. Parametrization of the differential cross section in the central region ($|\eta| < 1.4$) for prompt muons (solid line) and decay muons (dashed line).

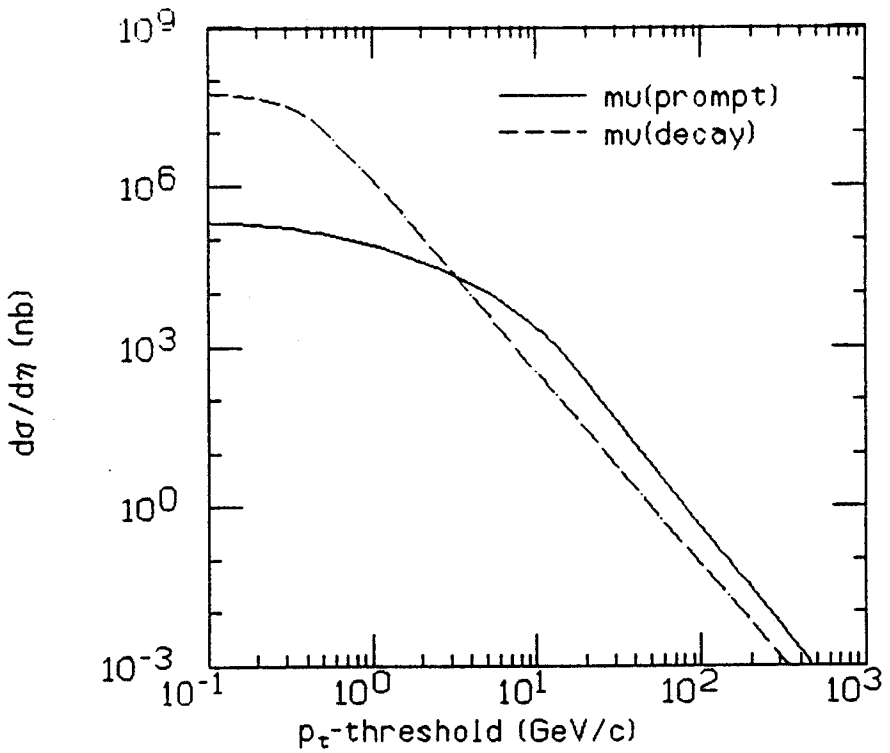

Fig.7. Integrated cross section in the central region ($|\eta| < 1.4$) as a function of p_t-threshold for prompt muons (solid line) and decay muons (dashed line).

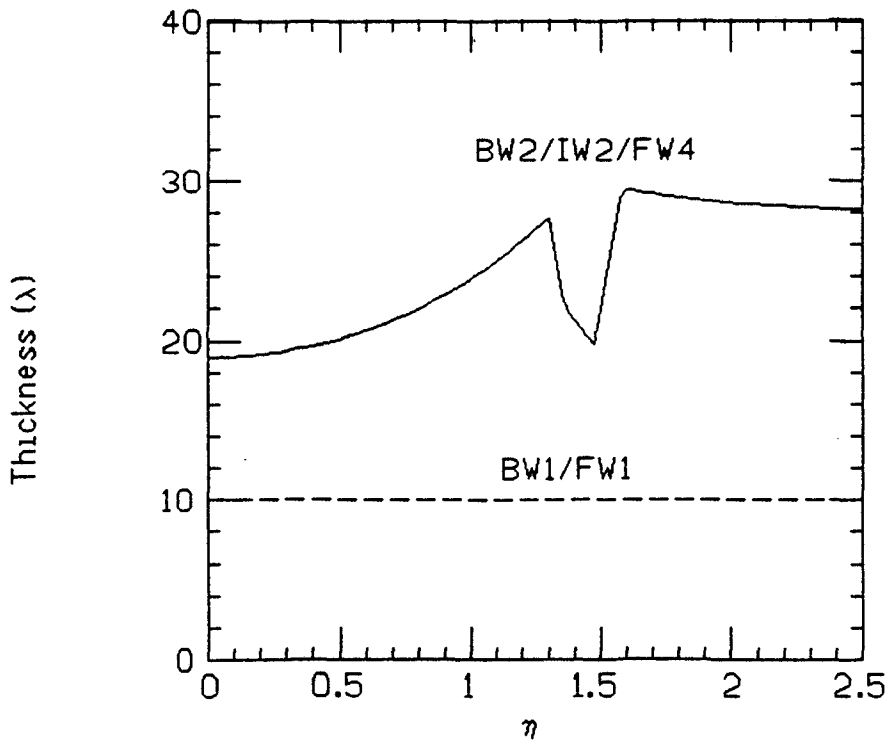

Fig.8. Material thickness up to BW1/FW1 (dashed line) and BW2/IW2/FW4 (solid line) in interaction length. The thickness of the calorimeter and materials inside is assumed to be 10 λ independent of η.

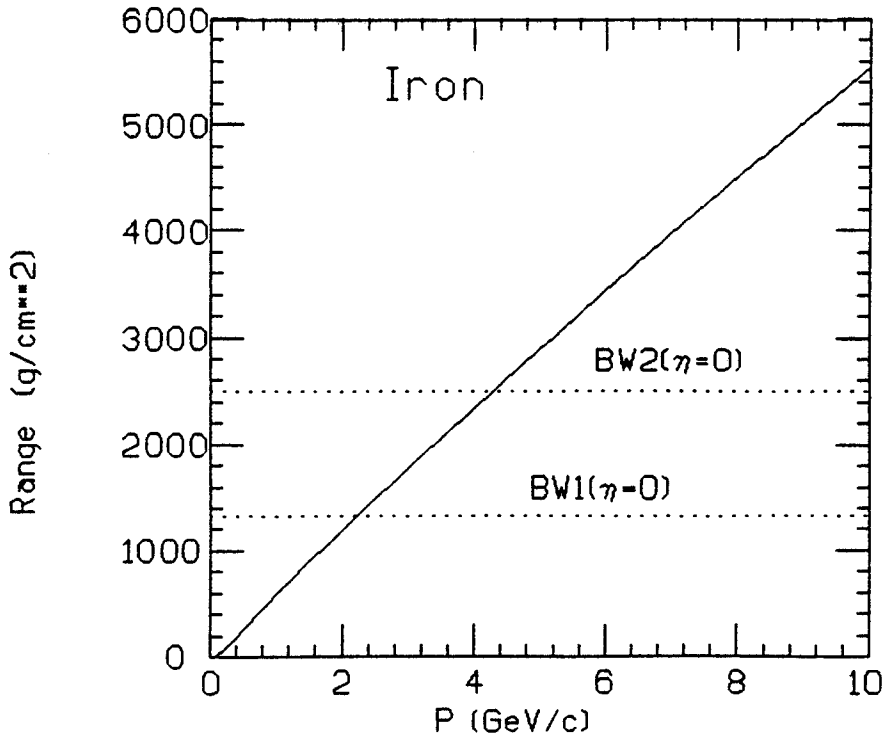

Fig.9. Muon range in iron as a function of momentum.

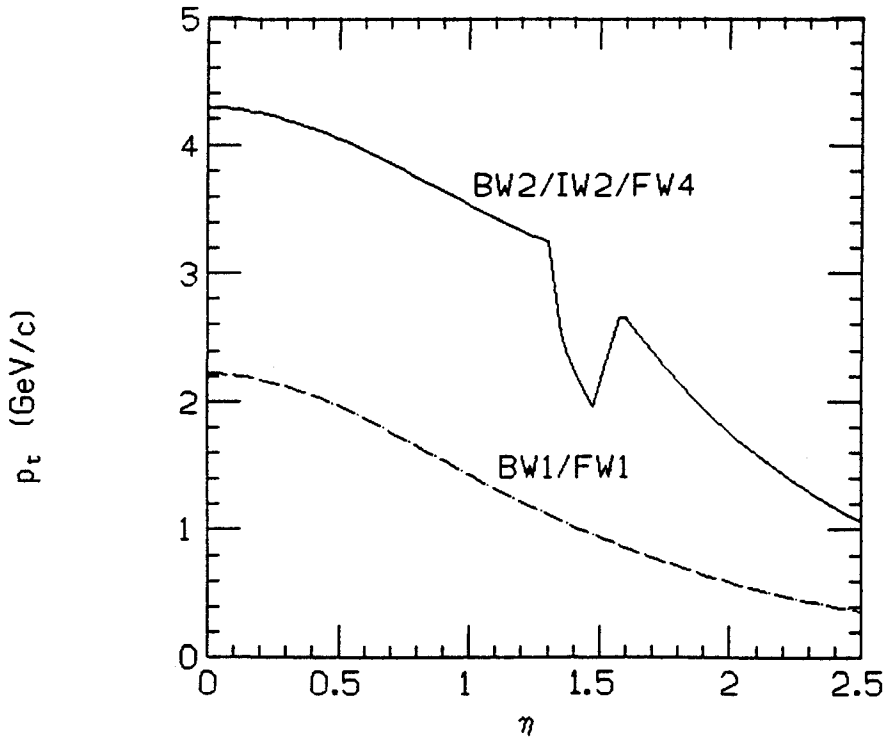

Fig.10. Minimum p_t required to penetrate the calorimeter (dashed line) or the iron toroid (solid line) as a function of η.

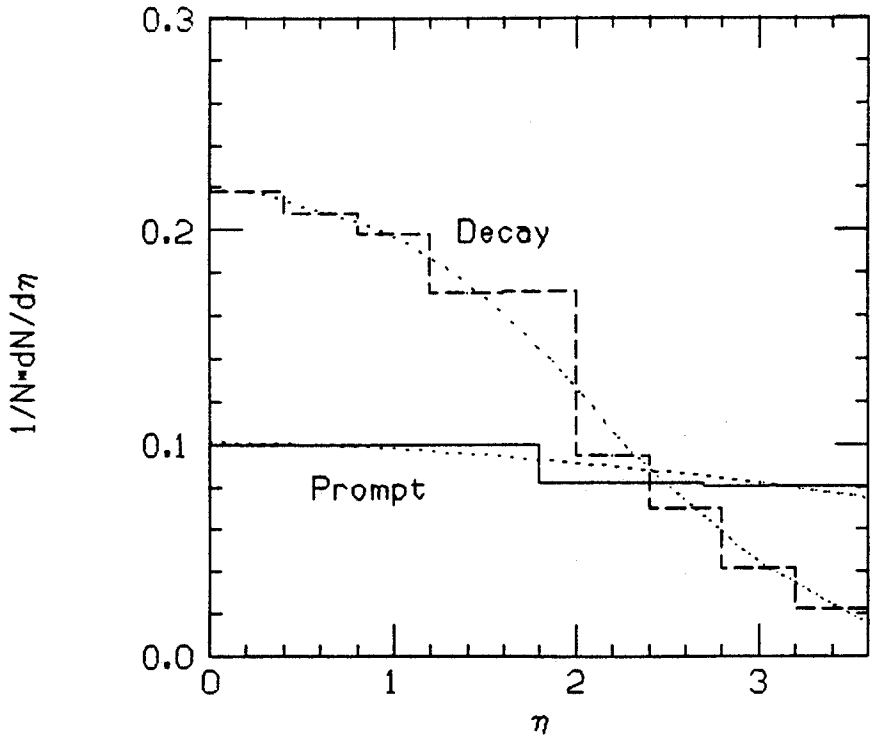

Fig.11. Parametrization of the pseudorapidity distribution of prompt muons and decay muons. Histogram with solid (dashed) line is the distribution of the prompt (decay) muons shown in Fig.4 (Fig.14) with $p_t > 1$ GeV/c.

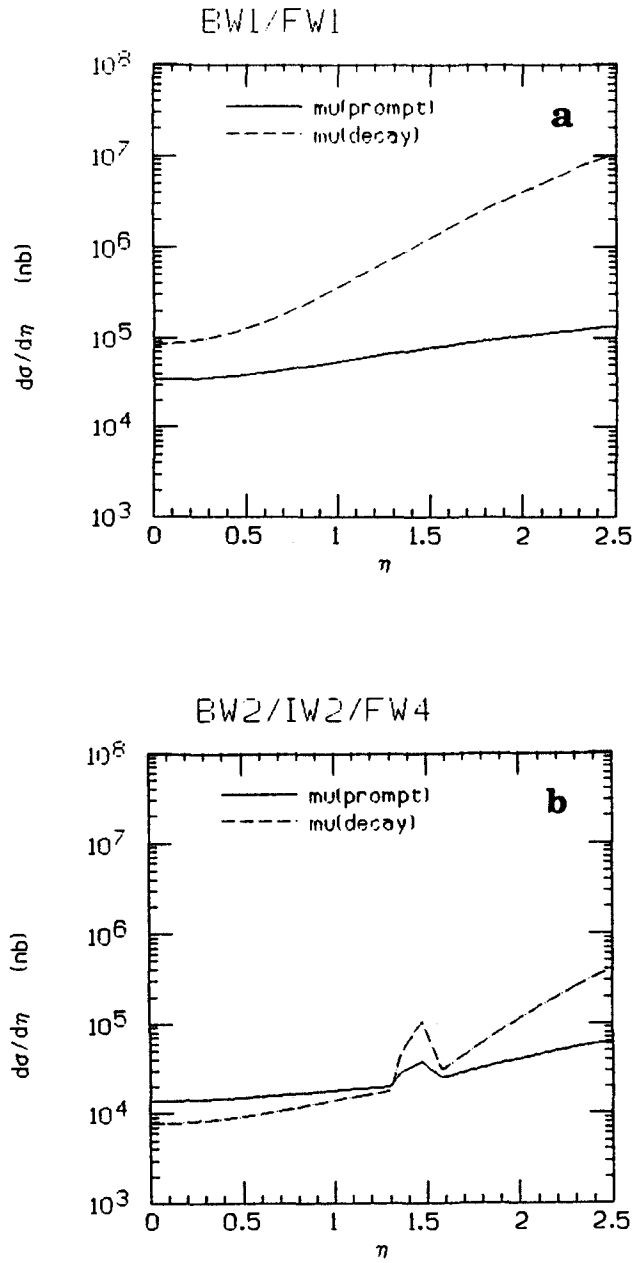

Fig. 12. Differential cross section, ds/dη, as a function of η for prompt muons (solid line) and decay muons (dashed line) at BW1/FW1 (a), and at BW2/IW2/FW4 (b).

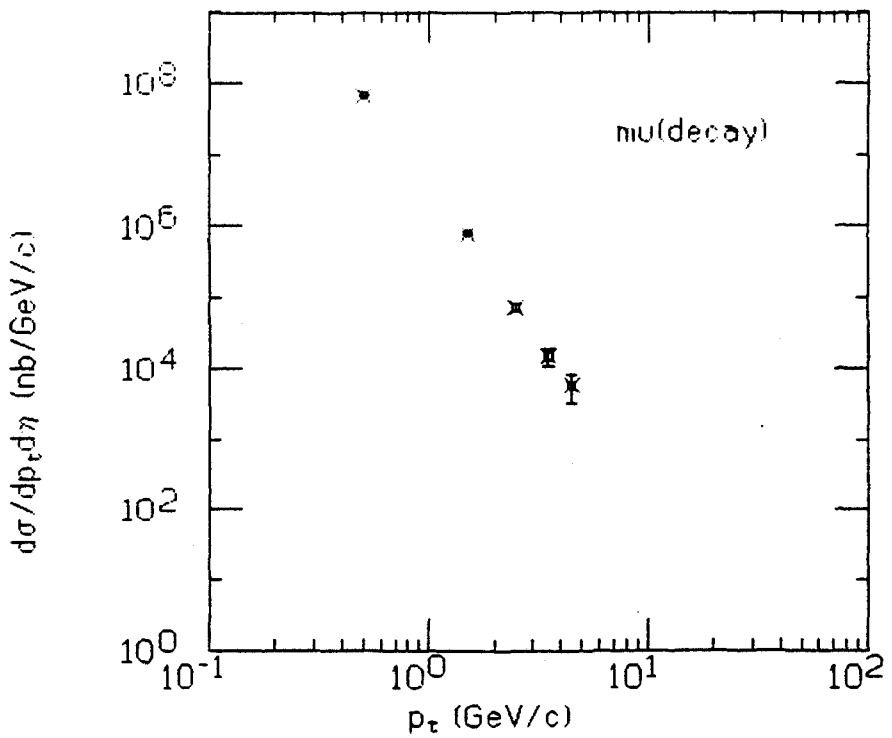

Fig.13. Differential cross section, $ds/dp_t\, d\eta$, as a function of p_t for decay muons. Events are generated by using PYTHIA5.3.

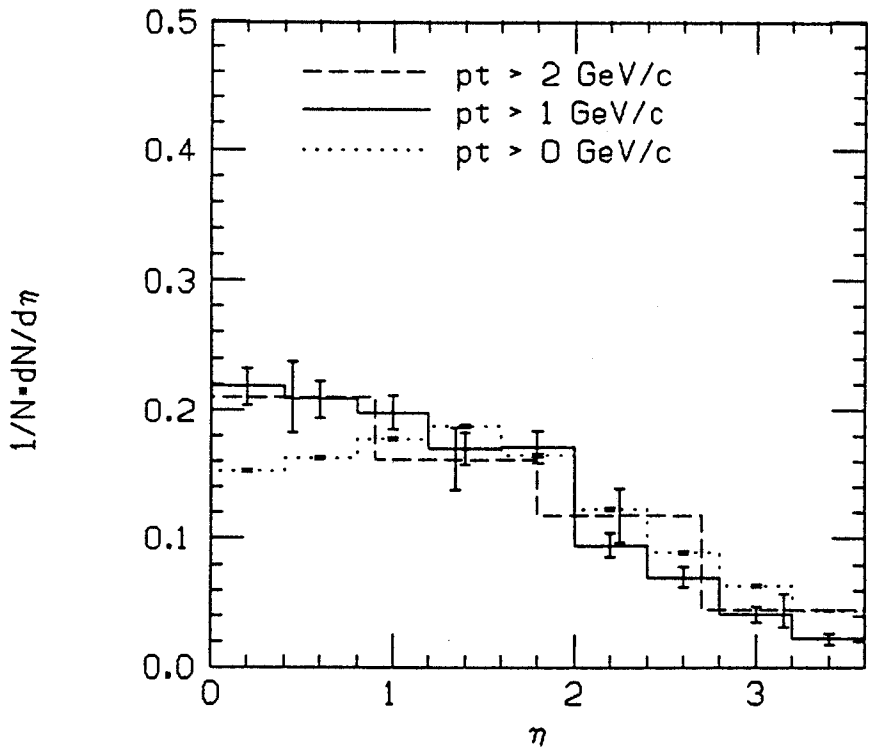

Fig.14. Pseudorapidity distribution for any decay muons (dotted line), those with p_t larger than 1 GeV/c (solid line) or 2 GeV/c (dashed line).

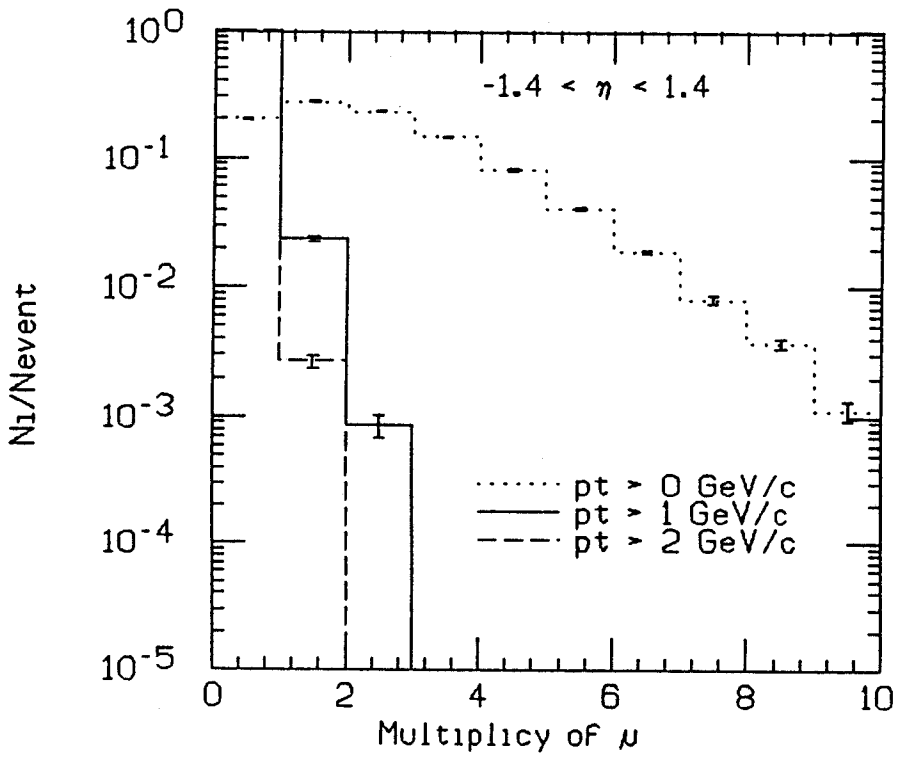

Fig.15. Multiplicity distribution of decay muons which enter the central region ($|\eta| < 1.4$) for any decay muons (dotted line), those with p_t larger than 1 GeV/c (solid line) or 2 GeV/c (dashed line).

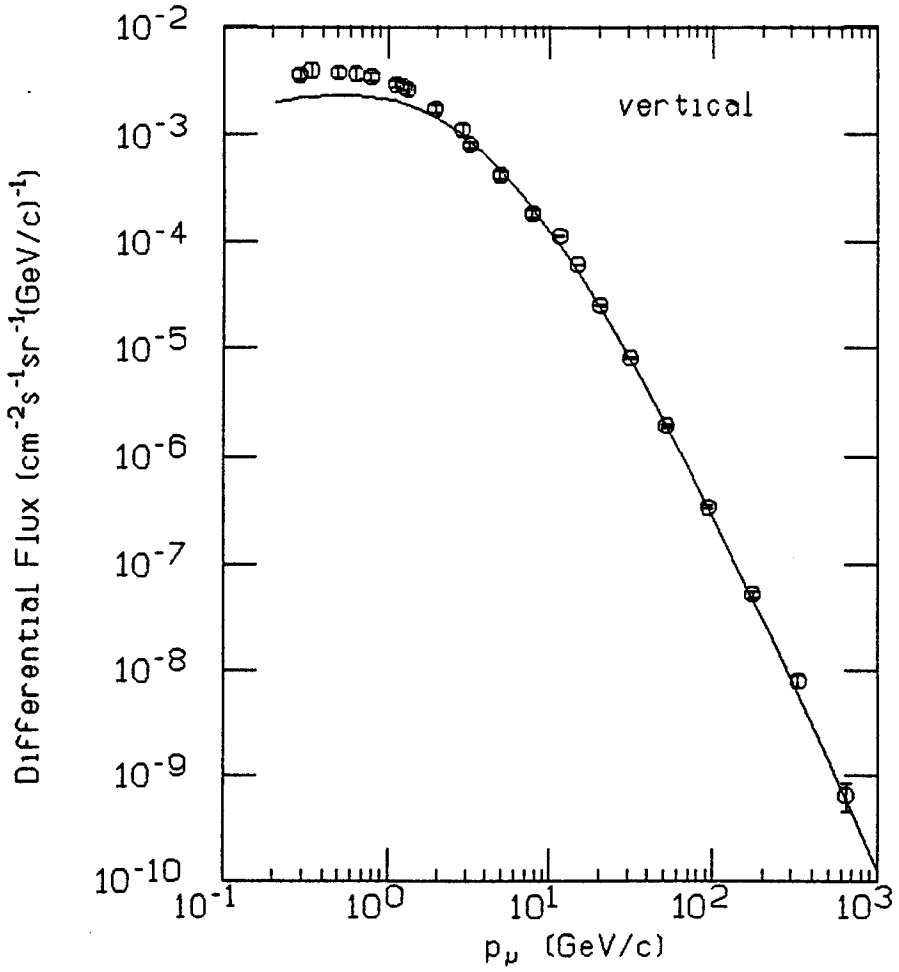

Fig.16. Differential flux in the vertical direction calculated with the formula given in ref.[7] together with experimental data points (open circle).

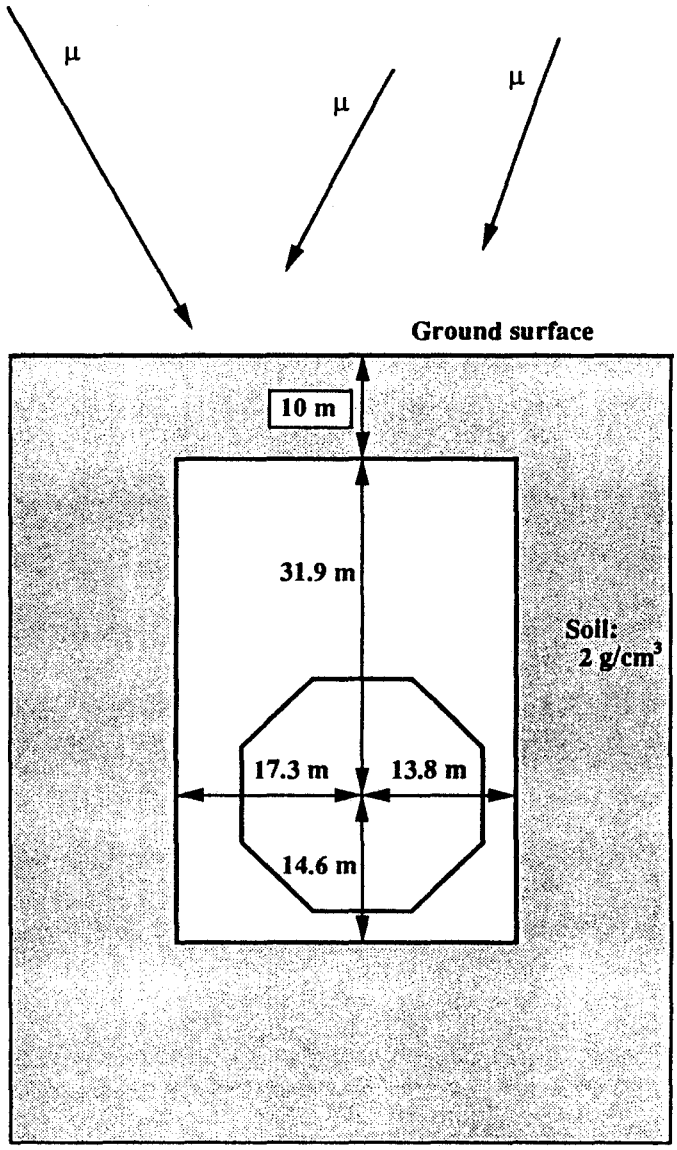

Fig.17. Cross-sectional view of the simplified experimental hall.